HHS Public Access

Author manuscript

Exp Eye Res. Author manuscript; available in PMC 2023 July 01.

Published in final edited form as:

Exp Eye Res. 2022 July ; 220: 109112. doi:10.1016/j.exer.2022.109112.

ECM stiffness modulates the proliferation but not the motility of primary corneal keratocytes in response to PDGF-BB

Krithika S. Iyer[1], **Daniel P. Maruri**[1], **Kara E. Peak**[1], **David W. Schmidtke**[1], **W. Matthew Petroll**[2], **Victor D. Varner**[1,3,*]

[1]Department of Bioengineering, University of Texas at Dallas, Richardson, TX

[2]Department of Ophthalmology, UT Southwestern Medical Center, Dallas, TX

[3]Department of Surgery, UT Southwestern Medical Center, Dallas, TX

Abstract

During corneal wound healing, keratocytes present within the corneal stroma become activated into a repair phenotype upon the release of growth factors, such as transforming growth factor-beta 1 (TGF-β1) and platelet-derived growth factor-BB (PDGF-BB). The process of injury and repair can lead to changes in the mechanical properties of the tissue, and previous work has shown that the TGF-β1-mediated myofibroblast differentiation of corneal keratocytes depends on substratum stiffness. It is still unclear, however, if changes in stiffness can modulate keratocyte behavior in response to other growth factors, such as PDGF-BB. Here, we used a polyacrylamide (PA) gel system to determine whether changes in stiffness influence the proliferation and motility of primary corneal keratocytes treated with PDGF-BB. In the presence of PDGF-BB, cells on stiffer substrata exhibited a more elongated morphology and had higher rates of proliferation than cells in a more compliant microenvironment. Using a freeze-injury to assay cell motility, however, we did not observe any stiffness-dependent differences in the migration of keratocytes treated with PDGF-BB. Taken together, these data highlight the importance of biophysical cues during corneal wound healing and suggest that keratocytes respond differently to changes in ECM stiffness in the presence of different growth factors.

Keywords

Corneal wound healing; mechanobiology; biomechanics; freeze injury; platelet-derived growth factor

Introduction

The cornea is the soft transparent tissue located at the anterior aspect of the eye (Andresen et al., 1997). It refracts light towards the retina and contains three cellular layers: an epithelium, endothelium, and stroma. The stromal compartment accounts for the bulk of the corneal thickness (Hahnel et al., 2000) and contains a highly organized extracellular matrix

*Address correspondence to V.D.V., University of Texas at Dallas, 800 W Campbell Rd., BSB 13.806, Tel: 972-883-7203, vdv@utdallas.edu.

(ECM) that consists of lamellae of aligned type I collagen fibrils (Hogan et al., 1971; Meek, 2009). This lattice-like microstructure reduces the scattering of light and endows the tissue, in part, with its optically transparent properties (Hassell and Birk, 2010).

A population of cells called corneal keratocytes reside within the stromal compartment (Fini, 1999; Nishida et al., 1988). In the healthy cornea, these cells form a relatively sparse network and are interconnected by numerous dendritic cellular extensions (Hassell and Birk, 2010; Jester et al., 1994). In this mechanically quiescent state, keratocytes are primarily responsible for maintaining the highly ordered ECM within the corneal stroma (Beales et al., 1999; Jester et al., 1994; Zieske et al., 2001). Following injury, however, these cells differentiate into fibroblasts or myofibroblasts and attempt to repair the wound (Fini, 1999). This process is driven, in part, by the release of growth factors and cytokines into the stromal space, which include both transforming growth factor beta-1 (TGF-β1) and platelet derived growth factor-BB (PDGF-BB), among others (Imanishi et al., 2000; Torricelli et al., 2013; Wilson et al., 2001). TGF-β1 promotes the myofibroblast differentiation of corneal keratocytes (Jester et al., 1999; Kurosaka et al., 1998; Nakamura, 2003), while PDGF-BB stimulates the motility and proliferation of keratocytes to repopulate the wound (Kim et al., 2009). Although normal corneal wound healing largely regenerates the complex architecture of the tissue, at times, this process can elicit a protracted fibrotic response, which distorts the stromal ECM and creates optical defects, such as corneal hazing (Boote et al., 2012; Chen et al., 2000; Singh et al., 2012).

Previous work has suggested that the mechanical properties of the cornea undergo significant changes during wound healing, with the tissue stiffening substantially in the days following an injury (Raghunathan et al., 2017; Thomasy et al., 2014). These changes in mechanical properties have been shown to influence the TGF-β1-mediated myofibroblast differentiation of corneal keratocytes (Kim et al., 2009; Maruri et al., 2020), but it is unclear if they also regulate the behavior of keratocytes in response to other growth factors, such as PDGF- BB. To address this question, we used a polyacrylamide (PA) gel system to create collagen-coated substrata of different stiffnesses (Lee et al., 2012; Simi et al., 2018), which approximate the mechanical properties of either normal or fibrotic corneal tissue (Kim et al., 2020; Raghunathan et al., 2017; Thomasy et al., 2014; Winkler et al., 2011). These gels were then plated with primary normal rabbit keratocytes (NRKs) and cultured in the presence or absence of PDGF-BB to determine how changes in ECM compliance influence the motility and proliferation of corneal keratocytes in response to PDGF-BB.

Methods

Fabrication of polyacrylamide (PA) gels

PA substrata of varying stiffnesses were fabricated on surface-treated glass coverslips, as described previously (Lee et al., 2012; Maruri et al., 2020; Simi et al., 2018). Briefly, a small volume (~40 μl) of unpolymerized PA solution was sandwiched between two silanized 30 mm diameter glass coverslips and allowed to polymerize under vacuum for 30 min. The top coverslip was then removed using fine forceps, and the surface of the gel was functionalized using the heterobifunctional cross-linker sulfo-SANPAH (Pierce Biotechnology, Rockford, IL), as well as a 50 μg/ml solution of bovine type I collagen

(PureCol; Advanced Biomatrix, San Diego, CA). The mechanical properties of the gel were modulated by altering the concentrations of acrylamide (Bio-Rad, Hercules, CA) and bis-acrylamide (Bio-Rad, Hercules, CA) in the pre-polymerization solution. We used 7.5% acrylamide and 3.0% bis-acrylamide to fabricate 1 kPa (soft) gels and 12.5% acrylamide and 17.5% bis-acrylamide to fabricate 10 kPa (stiff) gels. As controls, we also fabricated collagen-coated glass coverslips, as described previously (Kivanany et al., 2018; Miron-Mendoza et al., 2015). Briefly, untreated glass coverslips were incubated in a neutralized 50 μg/ml solution of bovine type I collagen at 37°C for 30 min and then rinsed twice with Dulbecco's modified Eagle's medium (DMEM; Sigma-Aldrich, St. Louis, MO).

Cell culture and reagents

Primary normal rabbit keratocytes (NRKs) were isolated from New Zealand white rabbit eyes (Pel Freez, Rogers, AR), as described previously (Jester et al., 1996; Jester and Ho-Chang, 2003; Lakshman et al., 2010). Briefly, corneal buttons were excised using surgical scissors, denuded of both the endothelium and epithelium, and incubated overnight at 37°C in digestion medium containing 0.5 mg/ml hyaluronidase (Worthington Biochemicals, Lakewood, NJ), 2 mg/ml collagenase (Gibco), and 2% penicillin/streptomycin/amphotericin B (Lonza, Walkersville, MD). Afterward, centrifuge-pelleted NRKs were then plated in tissue culture flasks and cultured at 37°C in serum-free medium containing DMEM supplemented with 1% RPMI vitamin mix (Sigma-Aldrich, St. Louis, MO), 100 μM nonessential amino acids (Invitrogen, Carlsbad, CA), 100 μg/ml ascorbic acid (Sigma-Aldrich, St. Louis, MO), and 1% penicillin/streptomycin/amphotericin B (Jester and Ho-Chang, 2003; Lakshman and Petroll, 2012).

First passage cells, cultured for 5 days in serum-free conditions, were used in all experiments. The cells were plated on both collagen-functionalized PA gels and collagen-coated glass coverslips at a density of either 15,000 cells/ml or 30,000 cells/ml, depending on the experiment. (The lower cell density was used to avoid any errors owing to cell-cell overlap when comparing the morphology of cultured NRKs.) In all experiments, keratocytes were maintained in serum-free conditions for 48 hr after plating to enable cell attachment. Then either 50 ng/ml PDGF-BB (Gibco) or vehicle control (100 mM acetic acid containing 0.1% BSA solution) was added to the medium, and the cells were cultured for an additional 72 hr.

Fluorescence microscopy and staining

Cells were fixed in 3% paraformaldehyde in phosphate-buffered saline (PBS) and washed 3 times with PBS. Fixed samples were then permeabilized in 0.5% Triton X-100 in PBS for 30 min at room temperature and blocked with 1% bovine serum albumin fraction V (Equitech-Bio, Kerrville, TX) in PBS for 30 min at room temperature. The Click-iT EdU Imaging Kit (Invitrogen; Carlsbad, CA) was used to detect cells in S-phase. Cells were pulsed with EdU 72 hr prior to fixation. After fixation, samples were washed three times in PBS and then incubated with Alexa Fluor 488 phalloidin (1:400 dilution) (Invitrogen, Carlsbad, CA) for 2 hr at 37°C, washed three times, and then incubated with 4'−6-diamidino- 2-phenylindole (DAPI; 1:1000 dilution) (Sigma-Aldrich; St. Louis, MO) at room temperature for 20 min. Confocal microscopy of fixed samples was performed on a Zeiss LSM 800 laser scanning

confocal microscope, equipped with a motorized stage and controlled by Zen 2.3 (blue edition) software. Images were taken using a 10×, NA 0.30, EC Plan-Neofluar objective (Zeiss). Wide-field fluorescence images were captured of some samples using a Zeiss AxioVert microscope with a 5×, NA 0.15, LD A-Plan (Ph1) objective (Zeiss). Morphometric analysis of cell geometry was performed using the Analyze Particles plugin in ImageJ, as described previously (Maruri et al., 2020), or using either the Hull and Circle plugin (to measure convex hull area) or the Cell Counter plugin (to count the number of dendritic cellular processes). Keratocyte proliferation was quantified using the ratio of EdU^+/DAPI-stained nuclei.

Freeze injury assay

In other experiments, we used a freeze injury assay to determine the effect of substratum stiffness on PDGF-BB-induced cell motility. As described previously (Kivanany et al., 2018), we used a liquid nitrogen-cooled rod, held to the bottom of the culture dish, to create a freeze injury within a confluent layer of NRKs. Briefly, we plated cells at a density of 75,000 cells/ml (15,750 cells/cm^2) in each well of a customized multi-well plate, containing either collagen-functionalized PA substrata or collagen-coated glass coverslips. Cells were maintained in serum-free conditions for 48 hr to enable cell attachment. Then the culture medium was removed, and a liquid nitrogen-cooled rod (~1.5 mm in diameter) was held to the underside of each well for 15 s, to create a circular freeze injury on each substratum. Any detached cells were washed away with serum-free medium, and the area was inspected visually using a phase-contrast microscope to ensure that cells had detached from the wound area. Following the injury, either serum-free medium or medium supplemented with 50 ng/ml PDGF-BB was added to each well, and the multi-well plate was transferred to a humidified stage-top incubator, situated atop a Zeiss AxioObserver 7 microscope and cultured for 96 hr at 37°C. Phase-contrast images of the entire wound area were captured at 1 hr intervals in each well. Then, at the end of the experiment, cell nuclei were stained with Hoechst (1:1000 dilution; Invitrogen, Carlsbad, CA) to determine the locations of cells in the injury after 96 hr of culture.

Cell migration into the wound was quantified in three ways. First, the distance of each Hoechst-stained nucleus from the initial wound border (d_n) was calculated for all cells within the injury (after 96 hr of culture) using the following equation:

$$d_n = r - \sqrt{(x_n - x_c)^2 + (y_n - y_c)^2}$$

where r is the initial radius of the wound, (x_n, y_n) represents the Cartesian coordinates of each Hoechst-stained nucleus, and (x_c, y_c) gives the Cartesian coordinates of the center of the circular wound (Fig. S1). We also used the time-lapse phase contrast images to (i) track the motion of the leading edge of the wound and (ii) track the motion of individual cells migrating into the wound. All tracking analyses were performed using the Manual Tracking plugin in ImageJ.

Microindentation testing

We used the MicroSquisher mechanical testing system to perform microindentation experiments of PA substrata before and after the creation of a freeze injury. This device uses an actuator-controlled cantilever beam, affixed to an indenter tip of known geometry, to apply a compressive force to the material. Soft and stiff PA gels were mechanically tested using a 76 μm-diameter cylindrical indenter. The applied force F and gel deflection . were measured as functions of time. The resultant force-deflection (F-δ) curves were then used to estimate the Young's modulus of the gel via the following equation (Harding and Sneddon, 1945; McKee et al., 2011):

$$E = \frac{F\left(1 - v^2\right)}{2R\delta}$$

where E and v represent the Young's modulus and Poisson's ratio of the gel, respectively, F is the applied force, R indicates the radius of the indenter, and δ is deflection of the gel.

Statistical Analysis

Data represents mean ± standard deviation from at least three experimental replicates. Statistical comparisons were made in Prism 9 (GraphPad; San Diego, CA) using a two-way ANOVA followed by a Tukey post-hoc test, with p-values as specified in the figure captions.

Results

Substratum stiffness modulates keratocyte morphology in the presence of PDGF-BB

We cultured primary corneal keratocytes on substrata of different stiffnesses in either the presence or absence of PDGF-BB. PA substrata with an elastic modulus of either 1 kPa (soft) or 10 kPa (stiff) were fabricated to approximate the mechanical properties of either normal (1.1 ± 0.6 kPa; Thomasy et al., 2014; Kim et al., 2020) or fibrotic corneal tissue (5.3 ± 2.3 kPa; Raghunathan et al., 2017), respectively. Collagen-coated glass coverslips (~GPa) were used as controls (Jester et al., 2002, 1999; Kivanany et al., 2018; Miron-Mendoza et al., 2015). In serum-free conditions, on all substrata, the cultured NRKs retained the branched, dendritic morphology indicative of mechanically quiescent keratocytes, with cortically localized F-actin, similar to that observed previously (Lakshman et al., 2010) (Fig. 1A). After 72 hr of culture in PDGF-BB-containing medium, however, the keratocytes exhibited striking changes in shape, with the cells possessing a more spread out and elongated morphology (Fig. 1B–C). Consistent with previous studies (Gallego-Muñoz et al., 2017; Haber et al., 2003; Kim et al., 2009; Lakshman and Petroll, 2012) treatment with PDGF-BB did not promote the formation of stress fibers; instead, similar to cells in serum-free conditions, the cultured NRKs retained predominantly cortical F-actin (Fig. 1B). Quantitative morphometric analysis of keratocyte geometry indicated significant stiffness-dependent increases in cell area, length, and elongation in the presence of PDGF-BB (Fig. 1D–G). In serum-free conditions, NRKs displayed numerous dendritic extensions, and although these decreased in number upon treatment with PDGF-BB, in neither case did we observe stiffness-dependent differences in the number of branched cellular processes (Fig. 1H).

Increases in substratum stiffness promote elevated proliferation in response to PDGF-BB

Since PDGF-BB has been shown to promote the proliferation of corneal keratocytes (Kim et al., 2009), we also quantified rates of EdU incorporation among NRKs cultured in either the presence or absence of PDGF-BB on substrata of varying stiffnesses (Fig. 2). In serum-free conditions, very few EdU^+ nuclei were observed on any substrata regardless of stiffness (Fig. 2A). After 3 days in PDGF-BB-containing medium, however, the cultured NRKs exhibited an increase in proliferation that depended on substratum stiffness (Fig. 2B–C). On substrata of each stiffness, the presence of PDGF-BB elicited a significant increase in the fraction of EdU^+ nuclei, as compared to serum-free conditions (Fig. 2D). However, among the cells treated with PDGF-BB, those which were cultured on the stiffest (~GPa) substrata exhibited the highest rates of proliferation (Fig. 2D), suggesting that increases in substratum stiffness can promote elevated proliferation within PDGF-BB-treated keratocytes.

PDGF-BB-treated keratocytes repopulate decellularized wounds regardless of substratum stiffness

PDGF-BB has also been shown to stimulate the motility of corneal keratocytes (Andresen et al., 1997; Gallego-Muñoz et al., 2017; Kim et al., 2009) and during corneal wound healing, is thought to promote the ingression of activated keratocytes into sites of injury (Gallego-Muñoz et al., 2017; Kivanany et al., 2018). To determine if changes in substratum stiffness influence the repopulation of cultured NRKs into a decellularized wound, we created circular freeze injuries, approximately 1.5 mm in diameter, within populations of keratocytes that were seeded to confluence on substrata of varying stiffnesses (Fig. 3A). The cells were then cultured for 96 hr in either the presence or absence of PDGF-BB. (In separate experiments, we confirmed that the freeze injury did not disrupt cell attachment (Fig. S2), nor modify the mechanical properties of the PA gel (Fig. S3)). In all treatment conditions, the NRKs migrated into the decellularized wound (Fig. 3B), and at the end of the experiment, we quantified the number of Hoechst-stained nuclei present within the initial wound area (Fig. 4). On substrata of all stiffnesses, the PDGF-treated cells more fully populated the decellularized zone (Fig. 4A–B). Histograms depicting the distance of cell nuclei from the initial wound border (Fig. 4C–D) revealed that, on substrata of all stiffnesses, a larger number of cells repopulated the wound in the presence, as opposed to the absence, of PDGF-BB (Fig. 4E). In addition, these PDGF-treated cells travelled further into the wound than their counterparts in serum-free conditions (Fig. 4F). However, we did not observe any stiffness-dependent differences in the number of PDGF-treated cells that had repopulated the freeze injury, nor in the distance they had travelled into the wound (Fig. 4E–F), a result which suggests that changes in substratum stiffness may not impact keratocyte migration in response to PDGF-BB.

PDGF-BB-treated keratocytes do not show stiffness-dependent differences in motility

To quantify the dynamics of wound closure more directly, in both the presence and absence of PDGF-BB, we also tracked the motion of the leading edge of the wound on substrata of different stiffnesses (Fig. 5; Movies S1–S6). We considered thin strips, oriented perpendicular to the wound border as regions of interest (Fig. 5A–B) and measured the displacement of the leading edge at different time-points over 96 hr of culture (Fig. 5C–

D). In all treatment conditions, the leading edge advanced approximately linearly in time (Fig. 5E), and on each type of substratum, the leading edge progressed more quickly when the NRKs had been treated with PDGF-BB (Fig. 5C–E). Linear regression analysis of edge displacement vs. time allowed us to compare the speed of the leading edge across multiple experimental replicates. On substrata of all stiffnesses, the speed of the leading edge was greater when cells had been exposed to PDGF-BB, but we did not observe any stiffness-dependent differences in the motion of the wound border in either the presence or the absence of PDGF-BB (Fig. 5F).

During these experiments, we noticed that most cells did not move unidirectionally toward the center of the wound (Movies S1–S6). Thus, it remained a possibility that individual cells might be exhibiting stiffness-dependent migration speeds, even though the aggregate motion of the leading edge was unaffected. To account for this possibility, we tracked the motion of individual cells during wound closure on substrata of different stiffnesses (Fig. 6). In all treatment conditions, the cells moved generally towards the decellularized wound region but followed wandering, peripatetic trajectories of variable length (Fig. 6A–B). In serum-free conditions, on substrata of all stiffnesses, the tracks were relatively short, with cells typically travelling only a small distance from the wound border (Fig. 6A). But in the presence of PDGF-BB, individual keratocytes traveled substantially further into the decellularized region (Fig. 6B). Quantification of average cell speed revealed that, although PDGF-BB-treated cells migrated more quickly than their counterparts in serum-free conditions, no stiffness-dependent differences in cell motility were present (Fig. 6C). Taken together, these results suggest that changes in substratum stiffness do not alter the migratory phenotype of corneal keratocytes in the presence of PDGF-BB.

Discussion

PDGF can be expressed in one of several different isoforms (Fredriksson et al., 2004; Ross et al., 1986), and signaling downstream of PDGF has been shown to promote cell proliferation, contractility, and chemotaxis in a variety of different cell types (Grinnell, 2000; Hoch and Soriano, 2003). In the cornea, PDGF-BB is expressed within the corneal epithelium (Kim et al., 1999) and is also present in tear fluid (Tuominen et al., 2001; Vesaluoma et al., 2009). Following an injury, PDGF-BB is released into the stromal compartment and is thought to stimulate the migration and mitosis of corneal keratocytes (Kamil and Mohan, 2020; Kim et al., 2009; Wilson et al., 2003). Consistent with this idea, treatment with PDGF-BB has been shown to promote a more elongated keratocyte morphology in culture (Jester and Ho-Chang, 2003), as well as increases in both cell proliferation (Denk and Knorr, 1997; Kim et al., 1999) and motility (Andresen et al., 1997; Andresen and Ehlers, 1998; Kim et al., 2009).

In addition, wound healing is also associated with changes in corneal stiffness (Raghunathan et al., 2017), and increased substratum stiffness has been shown to regulate the TGF-β1-mediated myofibroblast differentiation of cultured keratocytes (Dreier et al., 2013; Maruri et al., 2020; Petroll et al., 2020). It is still unclear, however, if the mechanical properties of the ECM impact keratocyte behavior in response to other growth factors, such as PDGF-BB. Here, we investigated whether changes in substratum stiffness influence the

morphology, proliferation, and motility of PDGF-BB-treated primary corneal keratocytes. Using a polyacrylamide gel system, we demonstrated that elevated stiffness promotes increased cell spreading and elongation, and stimulates higher levels of PDGF-BB-driven proliferation. We did not, however, observe any stiffness-dependent differences in the motility of PDGF-BB-treated keratocytes using a freeze injury model of corneal wound healing.

Several previous studies have noted that both corneal fibroblasts and keratocytes form very few stress fibers and adopt elongated morphologies in the presence of PDGF-BB (Feng et al., 2017; Jester and Ho-Chang, 2003; Petroll and Lakshman, 2015). When cultured in either compressed or uncompressed 3D collagen gels, which have strikingly divergent mechanical properties (Barocas et al., 1995; Brown et al., 2005; Miron-Mendoza et al., 2012), PDGF-BB-treated keratocytes become highly elongated and extend numerous dendritic processes into the surrounding matrix (Petroll and Lakshman, 2015). Here, we have shown that the extent of PDGF-BB-induced cell spreading can be modulated by changes in substratum stiffness. Experiments using cultured corneal fibroblasts have suggested that cell spreading in response to PDGF-BB is associated with the activation of Rac (Petroll et al., 2008), but it remains unclear if Rac activity in corneal keratocytes varies with substratum stiffness. Consistent with this possibility, Rac inhibition of PDGF-BB-treated keratocytes has been shown to induce different phenotypes in uncompressed (soft) versus compressed (stiff) collagen matrices (Petroll and Lakshman, 2015). Although the effective collagen concentration also varies with stiffness in these matrices, this result suggests that variations in Rac activity may contribute to stiffness-dependent differences in keratocyte spreading.

We also found that changes in substratum stiffness can modulate rates of proliferation in NRKs treated with PDGF-BB. In vivo, keratocytes in the corneal stroma undergo apoptosis following an injury (Wilson et al., 1996), and an increase in the number of proliferating cells can be observed within the stroma of a healing wound (Mohan et al., 2003). Our data suggest that a stiffer microenvironment may promote elevated levels of proliferation in response to PDGF-BB, but it is unclear how the time-course of proliferating cells in vivo compares with temporal changes in tissue stiffness during corneal repair (Raghunathan et al., 2017). Interestingly, vascular smooth muscle cells have also been shown to undergo stiffness-dependent differences in PDGF-BB-mediated proliferation (Brown et al., 2010). In this case, changes in stiffness are associated with differences in the phosphorylation state of the PDGF receptor (PDGFR) (Brown et al., 2010). Changes in Rac activity, moreover, have also been linked to mechanosensitive proliferation in other cell types (Klein et al., 2009), and Rac inhibition has been shown to decrease the proliferation of corneal fibroblasts in culture (Chen et al., 2020). It would be interesting to determine whether stiffness-dependent differences in PDGFR and/or Rac activation regulate the proliferation of cultured primary keratocytes.

In contrast to proliferation, changes in substratum stiffness did not elicit differences in the migratory phenotype of PDGF-BB-treated keratocytes. Several previous studies, each using a distinct motility assay, have demonstrated that PDGF-BB promotes the migration of corneal fibroblasts and keratocytes (Gallego-Muñoz et al., 2017; Kim et al., 2009; Kivanany et al., 2018). Corneal stromal cells, however, exert only modest traction forces

in response to PDGF-BB, as assayed by either ECM compaction (Lakshman and Petroll, 2012) or by tracked fibril deformations in 3D collagen matrices (Petroll et al., 2008). This mechanical phenotype is consistent with that of other fibroblastic cell types. Chick embryonic fibroblasts, for instance, exert much smaller traction forces upon treatment with PDGF-BB than with either serum or lysophosphatidic acid (LPA) (Grinnell, 2000; Kolodney and Elson, 1993). Consistent with these data, PDGF-BB-treated keratocytes exhibit poorly formed focal adhesions (Jester et al., 2002), which, in other cell types, are associated with lower traction forces (Stricker et al., 2011). During corneal wound healing, it may be that migrating keratocytes do not exert large enough traction forces in the presence of PDGF-BB to exhibit stiffness-dependent differences in motility. Our experiments, however, consider only 2D migration, in which the cells do not need to proteolytically degrade the ECM to migrate efficiently, as they often need do in 3D matrices (Ehrbar et al., 2011). In addition, cultured keratocytes were not subjected to gradients of substratum stiffness, which have been shown to promote directed cell migration or durotaxis (Lo et al., 2000; Plotnikov and Waterman, 2013). It would be interesting to determine whether or not cultured keratocytes continue to exhibit stiffness-independent motility when cultured in 3D matrices with gradients in mechanical properties.

Even so, taken together, our data highlight the importance of ECM mechanics during corneal wound healing. Biophysical factors, such as tissue stiffness, can impact the behavior of corneal keratocytes in response to soluble growth factors other than TGF-β1. Changes in stiffness modulate the proliferation and spreading of NRKs treated with PDGF-BB, but not their migration into decellularized wounds. This difference in behavior suggests that distinct mechanotransductive pathways might regulate the proliferation and motility of corneal keratocytes treated with PDGF-BB. Future work, targeted at disentangling the signaling mechanisms that mediate mechanosensitive keratocyte phenotypes, will help identify new therapeutic strategies to promote effective corneal wound healing.

Supplementary Material

Refer to Web version on PubMed Central for supplementary material.

Acknowledgements

This work was supported by the NIH grants R01 EY030190 and P30 EY030413, as well as an unrestricted grant from Research to Prevent Blindness.

References

Andresen JL, Ehlers N, 1998. Chemotaxis of human keratocytes is increased by platelet-derived growth factor-BB, epidermal growth factor, transforming growth factor-alpha, acidic fibroblast growth factor, insulin-like growth factor-I, and transforming growth factor-beta. Curr. Eye Res. 17, 79–87. [PubMed: 9472475]

Andresen JL, Ledet T, Ehlers N, 1997. Keratocyte migration and peptide growth factors: the effect of PDGF, bFGF, EGF, IGF-I, aFGF and TGF-β on human keratocyte migration in a collagen gel. Curr. Eye Res. 16, 605–613. [PubMed: 9192171]

Barocas VH, Moon AG, Tranquillo RT, 1995. The fibroblast-populated collagen microsphere assay of cell traction force—part 2: measurement of the cell traction parameter. J. Biomech. Eng. 117, 161–170. [PubMed: 7666653]

Beales MP, Funderburgh JL, Jester JV, Hassell JR, 1999. Proteoglycan synthesis by bovine keratocytes and corneal fibroblasts: maintenance of the keratocyte phenotype in culture. Invest. Ophthalmol. Vis. Sci. 40, 1658–63. [PubMed: 10393032]

Boote C, Du Y, Morgan S, Harris J, Kamma-Lorger CS, Hayes S, Lathrop KL, Roh DS, Burrow MK, Hiller J, Terrill NJ, Funderburgh JL, Meek KM, 2012. Quantitative assessment of ultrastructure and light scatter in mouse corneal debridement wounds. Invest. Ophthalmol. Vis. Sci. 53, 2786–2795. [PubMed: 22467580]

Brown RA, Wiseman M, Chuo C-B, Cheema U, Nazhat SN, 2005. Ultrarapid engineering of biomimetic materials and tissues: fabrication of nano- and microstructures by plastic compression. Adv. Funct. Mater. 15, 1762–1770.

Brown XQ, Bartolak-Suki E, Williams C, Walker ML, Weaver VM, Wong JY, 2010. Effect of substrate stiffness and PDGF on the behavior of vascular smooth muscle cells: implications for atherosclerosis. J. Cell Physiol. 225, 115–122. [PubMed: 20648629]

Chen C, Michelini-Norris B, Stevens S, Rowsey J, Ren X, Goldstein M, Schultz G, 2000. Measurement of mRNAs for TGFβ and extracellular matrix proteins in corneas of rats after PRK. Invest. Ophthalmol. Vis. Sci. 41, 4108–16. [PubMed: 11095603]

Chen J, Backman LJ, Zhang W, Ling C, Danielson P, 2020. Regulation of keratocyte phenotype and cell Behavior by substrate Stiffness. ACS Biomater. Sci. Eng. 6, 5162–5171. [PubMed: 33455266]

Denk PO, Knorr M, 1997. The in vitro effect of platelet-derived growth factor isoforms on the proliferation of bovine corneal stromal fibroblasts depends on cell density. Graefes Arch. Clin. Ex. Ophthal. 235, 530–534.

Dreier B, Thomasy SM, Mendonsa R, Raghunathan VK, Russell P, Murphy CJ, 2013. Substratum compliance modulates corneal fibroblast to myofibroblast transformation. Invest. Ophthalmol. Vis. Sci. 54, 5901. [PubMed: 23860754]

Ehrbar M, Sala A, Lienemann P, Ranga A, Mosiewicz K, Bittermann A, Rizzi SC, Weber FE, Lutolf MP, 2011. Elucidating the role of matrix stiffness in 3D cell migration and remodeling. Biophys. J. 100, 284–293. [PubMed: 21244824]

Feng X, Pi L, Sriram S, Schultz GS, Gibson DJ, 2017. Connective tissue growth factor is not necessary for haze formation in excimer laser wounded mouse corneas. PLoS One 12, e0172304.

Fini ME, 1999. Keratocyte and fibroblast phenotypes in the repairing cornea. Prog. Retin. Eye Res. 18, 529–551. [PubMed: 10217482]

Fredriksson L, Li H, Eriksson U, 2004. The PDGF family: four gene products form five dimeric isoforms. Cytokine Growth Factor Rev. 15, 197–204. [PubMed: 15207811]

Gallego-Muñoz P, Ibares-Frías L, Valsero-Blanco MC, Cantalapiedra-Rodriguez R, Merayo-Lloves J, Martínez-García MC, 2017. Effects of TGFβ1, PDGF-BB, and bFGF, on human corneal fibroblasts proliferation and differentiation during stromal repair. Cytokine 96, 94–101. [PubMed: 28390267]

Grinnell F, 2000. Fibroblast–collagen-matrix contraction: growth-factor signalling and mechanical loading. Trends Cell Biol. 10, 362–365. [PubMed: 10932093]

Haber M, Cao Z, Panjwani N, Bedenice D, Li WW, Provost PJ, 2003. Effects of growth factors (EGF, PDGF-BB and TGF-β1) on cultured equine epithelial cells and keratocytes: implications for wound healing. Vet. Ophthalmol. 6, 211–217. [PubMed: 12950652]

Hahnel C, Somodi S, Weiss DG, Guthoff RF, 2000. The keratocyte network of human cornea: a three-dimensional study using confocal laser scanning fluorescence microscopy. Cornea 19, 185–193. [PubMed: 10746451]

Harding JW, Sneddon IN, 1945. The elastic stresses produced by the indentation of the plane surface of a semi-infinite elastic solid by a rigid punch. Math. Proc. Camb. Philos. Soc. 41, 16–26.

Hassell JR, Birk DE, 2010. The molecular basis of corneal transparency. Exp. Eye Res. 91, 326–335. [PubMed: 20599432]

Hoch RV, Soriano P, 2003. Roles of PDGF in animal development. Development 130, 4769–4784. [PubMed: 12952899]

Hogan MJ, Alvarado JA, Weddell JE, 1971. Histology of the human eye: an atlas and textbook. Saunders, Philadelphia, PA.

Imanishi J, Kamiyama K, Iguchi I, Kita M, Sotozono C, Kinoshita S, 2000. Growth factors: importance in wound healing and maintenance of transparency of the cornea. Prog. Retin. Eye Res. 19, 113–129. [PubMed: 10614683]

Jester JV, Barry PA, Lind GJ, Petroll WM, Garana R, Cavanagh HD, 1994. Corneal keratocytes: in situ and in vitro organization of cytoskeletal contractile proteins. Invest. Ophthalmol. Vis. Sci. 35, 730–43. [PubMed: 8113024]

Jester JV, Barry-Lane PA, Cavanagh HD, Petroll WM, 1996. Induction of α-smooth muscle actin expression and myofibroblast transformation in cultured corneal keratocytes. Cornea 15, 505–516. [PubMed: 8862928]

Jester JV, Ho-Chang J, 2003. Modulation of cultured corneal keratocyte phenotype by growth factors/cytokines control in vitro contractility and extracellular matrix contraction. Exp. Eye Res. 77, 581–592. [PubMed: 14550400]

Jester JV, Huang J, Barry-Lane PA, Kao WW, Petroll WM, Cavanagh HD, 1999. Transforming growth factor(beta)-mediated corneal myofibroblast differentiation requires actin and fibronectin assembly. Invest. Ophthalmol. Vis. Sci. 40, 1959–67. [PubMed: 10440249]

Jester JV, Huang J, Petroll WM, Cavanagh HD, 2002. TGFβ induced myofibroblast differentiation of rabbit keratocytes requires synergistic TGFβ, PDGF and integrin signaling. Exp. Eye Res. 75, 645–657. [PubMed: 12470966]

Kamil S, Mohan RR, 2020. Corneal stromal wound healing: Major regulators and therapeutic targets. Ocul Surf 19, 290–306. [PubMed: 33127599]

Kim A, Lakshman N, Karamichos D, Petroll WM, 2009. Growth factor regulation of corneal keratocyte differentiation and migration in compressed collagen matrices. Invest. Ophthalmol. Vis. Sci. 51, 864–75. [PubMed: 19815729]

Kim S, Jalilian I, Thomasy SM, Bowman MAW, Raghunathan VK, Song Y, Reinhart-King CA, Murphy CJ, 2020. Intrastromal injection of hyaluronidase alters the structural and biomechanical properties of the corneal stroma. Transl. Vis. Sci. Technol. 9, 21.

Kim WJ, Mohan RR, Mohan RR, Wilson SE, 1999. Effect of PDGF, IL-1alpha, and BMP2/4 on corneal fibroblast chemotaxis: expression of the platelet-derived growth factor system in the cornea. Invest. Ophthalmol. Vis. Sci. 40, 1364–72. [PubMed: 10359318]

Kivanany PB, Grose KC, Yonet-Tanyeri N, Manohar S, Sunkara Y, Lam KH, Schmidtke DW, Varner VD, Petroll WM, 2018. An in vitro model for assessing corneal keratocyte spreading and migration on aligned fibrillar collagen. J. Funct. Biomater. 9, 54. [PubMed: 30248890]

Klein EA, Yin L, Kothapalli D, Castagnino P, Byfield FJ, Xu T, Levental I, Hawthorne E, Janmey PA, Assoian RK, 2009. Cell-cycle control by physiological matrix elasticity and in vivo tissue stiffening. Curr. Biol. 19, 1511–1518. [PubMed: 19765988]

Kolodney MS, Elson EL, 1993. Correlation of myosin light chain phosphorylation with isometric contraction of fibroblasts. J. Biol. Chem. 268, 23850–23855. [PubMed: 8226923]

Kurosaka H, Kurosaka D, Kato K, Mashima Y, Tanaka Y, 1998. Transforming growth factor-beta 1 promotes contraction of collagen gel by bovine corneal fibroblasts through differentiation of myofibroblasts. Invest. Ophthalmol. Vis. Sci. 39, 699–704. [PubMed: 9538875]

Lakshman N, Kim A, Petroll WM, 2010. Characterization of corneal keratocyte morphology and mechanical activity within 3-D collagen matrices. Exp. Eye Res. 90, 350–359. [PubMed: 20025872]

Lakshman N, Petroll WM, 2012. Growth Factor Regulation of Corneal Keratocyte Mechanical Phenotypes in 3-D Collagen Matrices. Invest. Ophthalmol. Vis. Sci. 53, 1077–1086. [PubMed: 22247479]

Lee K, Chen QK, Lui C, Cichon MA, Radisky DC, Nelson CM, 2012. Matrix compliance regulates Rac1b localization, NADPH oxidase assembly, and epithelial–mesenchymal transition. Mol. Biol. Cell 23, 4097–4108. [PubMed: 22918955]

Lo CM, Wang HB, Dembo M, Wang YL, 2000. Cell movement is guided by the rigidity of the substrate. Biophys. J. 79, 144–52. [PubMed: 10866943]

Maruri DP, Miron-Mendoza M, Kivanany PB, Hack JM, Schmidtke DW, Petroll WM, Varner VD, 2020. ECM stiffness controls the activation and contractility of corneal keratocytes in response to TGF-β1. Biophys. J. 119, 1865–1877. [PubMed: 33080219]

McKee CT, Last JA, Russell P, Murphy CJ, 2011. Indentation versus tensile measurements of Young's modulus for soft biological tissues. Tissue Eng. Part B Rev. 17, 155–164. [PubMed: 21303220]

Meek KM, 2009. Corneal collagen—its role in maintaining corneal shape and transparency. Biophys. Rev. 1, 83–93. 10.1007/s12551-009-0011-x [PubMed: 28509987]

Miron-Mendoza M, Graham E, Kivanany P, Quiring J, Petroll WM, 2015. The role of thrombin and cell contractility in regulating clustering and collective migration of corneal fibroblasts in different ECM environments. Invest. Ophthalmol. Vis. Sci. 56, 2079–2090. [PubMed: 25736789]

Miron-Mendoza M, Lin X, Ma L, Ririe P, Petroll WM, 2012. Individual versus collective fibroblast spreading and migration: regulation by matrix composition in 3D culture. Exp. Eye Res. 99, 36–44. [PubMed: 22838023]

Mohan RR, Hutcheon AEK, Choi R, Hong J, Lee J, Mohan, Rajiv R, Ambrósio R, Zieske JD, Wilson SE, 2003. Apoptosis, necrosis, proliferation, and myofibroblast generation in the stroma following LASIK and PRK. Exp. Eye Res. 76, 71–87. [PubMed: 12589777]

Nakamura K, 2003. Interaction between injured corneal epithelial cells and stromal cells. Cornea 22, S35–S47. [PubMed: 14703706]

Nishida T, Yasumoto K, Otori T, Desaki J, 1988. The network structure of corneal fibroblasts in the rat as revealed by scanning electron microscopy. Invest. Ophthalmol. Vis. Sci. 29, 1887–90. [PubMed: 3192380]

Petroll WM, Lakshman N, 2015. Fibroblastic transformation of corneal keratocytes by Rac inhibition is modulated by extracellular matrix structure and stiffness. J. Funct. Biomater. 6, 222–240. [PubMed: 25874856]

Petroll WM, Ma L, Kim A, Ly L, Vishwanath M, 2008. Dynamic assessment of fibroblast mechanical activity during Rac-induced cell spreading in 3-D culture. J. Cell Physiol. 217, 162–171. [PubMed: 18452153]

Petroll WM, Varner VD, Schmidtke DW, 2020. Keratocyte mechanobiology. Exp. Eye Res. 200, 108228.

Plotnikov SV, Waterman CM, 2013. Guiding cell migration by tugging. Curr. Opin. Cell Biol. 25, 619–26. [PubMed: 23830911]

Raghunathan VK, Thomasy SM, Strøm P, Yañez-Soto B, Garland SP, Sermeno J, Reilly CM, Murphy CJ, 2017. Tissue and cellular biomechanics during corneal wound injury and repair. Acta Biomater. 58, 291–301. [PubMed: 28559158]

Ross R, Raines EW, Bowen-Pope DF, 1986. The biology of platelet-derived growth factor. Cell 46, 155–169. [PubMed: 3013421]

Simi AK, Anlas AA, Stallings-Mann M, Zhang S, Hsia T, Cichon MA, Radisky DC, Nelson CM, 2018. A soft microenvironment protects from failure of midbody abscission and multinucleation downstream of the EMT-promoting transcription factor Snail. Cancer Res. 78, 2277–2289. [PubMed: 29483094]

Singh V, Agrawal V, Santhiago MR, Wilson SE, 2012. Stromal fibroblast–bone marrow-derived cell interactions: Implications for myofibroblast development in the cornea. Exp. Eye Res. 98, 1–8. [PubMed: 22465408]

Stricker J, Aratyn-Schaus Y, Oakes PW, Gardel ML, 2011. Spatiotemporal constraints on the force-dependent growth of focal adhesions. Biophys. J. 100, 2883–2893. [PubMed: 21689521]

Thomasy SM, Raghunathan VK, Winkler M, Reilly CM, Sadeli AR, Russell P, Jester JV, Murphy CJ, 2014. Elastic modulus and collagen organization of the rabbit cornea: epithelium to endothelium. Acta Biomater. 10, 785–791. [PubMed: 24084333]

Torricelli AAM, Singh V, Santhiago MR, Wilson SE, 2013. The corneal epithelial basement membrane: structure, function, and disease. Invest. Ophthalmol. Vis. Sci. 54, 6390–6400. [PubMed: 24078382]

Tuominen ISJ, Tervo TMT, Teppo A-M, Valle TU, Grönhagen-Riska C, Vesaluoma MH, 2001. Human tear fluid PDGF-BB, TNF-α and TGF-β1 vs corneal haze and regeneration of corneal epithelium and subbasal nerve plexus after PRK. Exp. Eye Res. 72, 631–641. [PubMed: 11384151]

Vesaluoma M, Teppo A-M, Grönhagen-Riska C, Tervo T, 2009. Platelet-derived growth factor-BB (PDGF-BB) in tear fluid: a potential modulator of corneal wound healing following photorefractive keratectomy. Curr. Eye Res. 16, 825–831.

Wilson SE, He Y-G, Weng J, Li Q, McDowall AW, Vital M, Chwang EL, 1996. Epithelial injury induces keratocyte apoptosis: hypothesized role for the interleukin-1 system in the modulation of corneal tissue organization and wound healing. Exp. Eye Res. 62, 325–338. [PubMed: 8795451]

Wilson SE, Mohan, Rahul R, Mohan, Rajiv R, Ambrósio R, Hong J, Lee J, 2001. The corneal wound healing response: cytokine-mediated interaction of the epithelium, stroma, and inflammatory cells. Prog. Retin. Eye Res. 20, 625–637. [PubMed: 11470453]

Wilson SE, Netto M, Ambrósio R, 2003. Corneal cells: chatty in development, homeostasis, wound healing, and disease. Am. J. Ophthalmol. 136, 530–536. [PubMed: 12967809]

Winkler M, Chai D, Kriling S, Nien CJ, Brown DJ, Jester B, Juhasz T, Jester JV, 2011. Nonlinear optical macroscopic assessment of 3-D corneal collagen organization and axial biomechanics. Invest. Ophthalmol. Vis. Sci. 52, 8818. [PubMed: 22003117]

Zieske JD, Guimarães SR, Hutcheon AEK, 2001. Kinetics of keratocyte proliferation in response to epithelial debridement. Exp. Eye Res. 72, 33–39. [PubMed: 11133180]

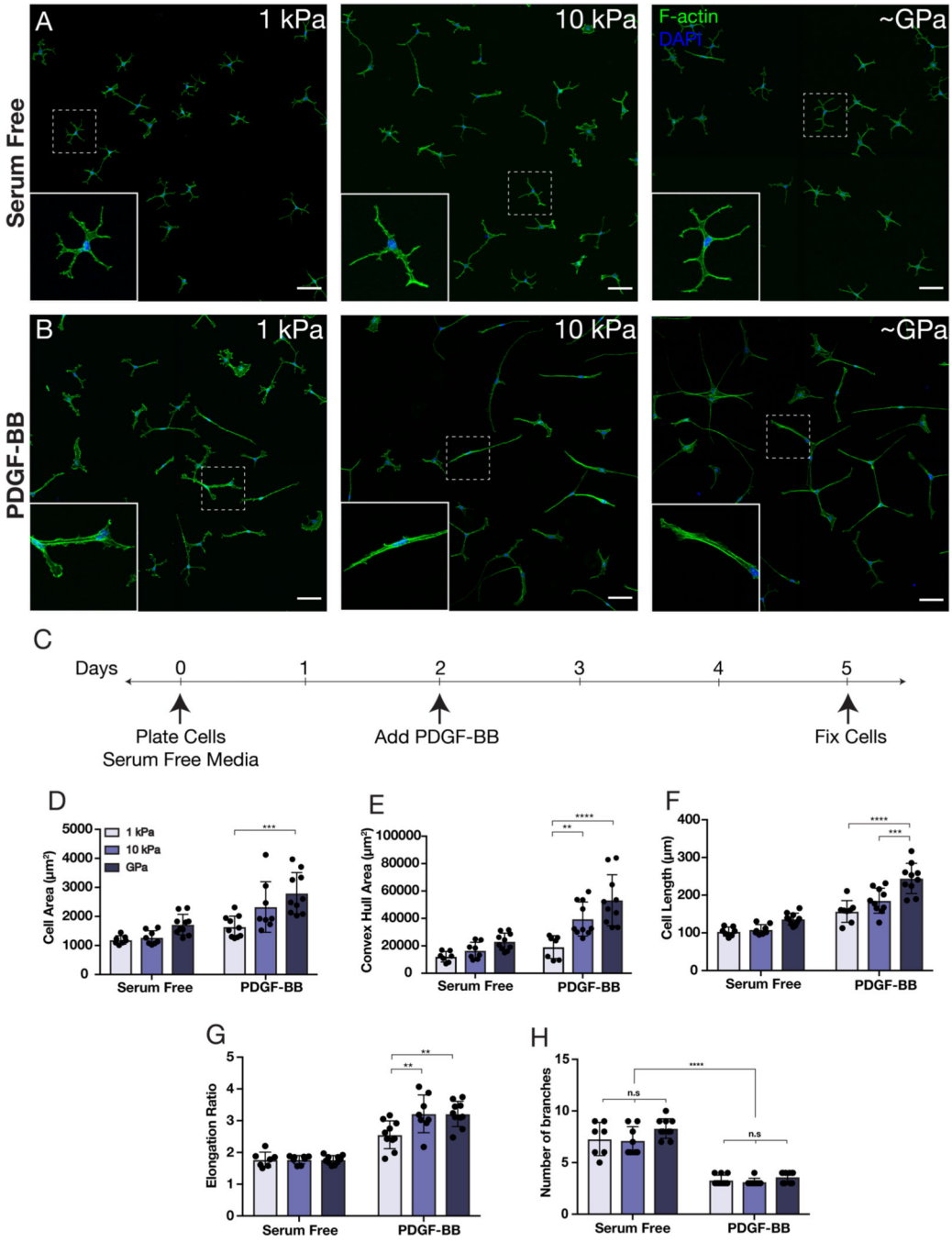

Fig. 1: Substratum stiffness influences the morphology of corneal keratocytes in the presence of PDGF-BB.

(A-B) Characteristic confocal fluorescence images of keratocytes cultured on either 1 kPa or 10 kPa PA substrata, or collagen-coated glass coverslips (~GPa). Cells were cultured in either (A) absence or (B) presence of PDGF-BB. Scale bars, 100 μm. (C) Experimental timeline. Keratocytes were fixed after 3 days of culture in PDGF-BB-containing medium. (D-H) Quantification of keratocyte morphology. Morphometric analysis of (D) projected cell area, (E) convex hull area, (F) cell length, (G) cell elongation, and (H) number of branched cellular projections. Error bars represent mean ± s.d. for n = 10 substrates from

5 experimental replicates. A two-way ANOVA with a Tukey post-hoc test was used to evaluate significance among groups (**, $p < 0.01$; ***, $p < 0.001$; ****, $p < 0.0001$; n.s., not significant).

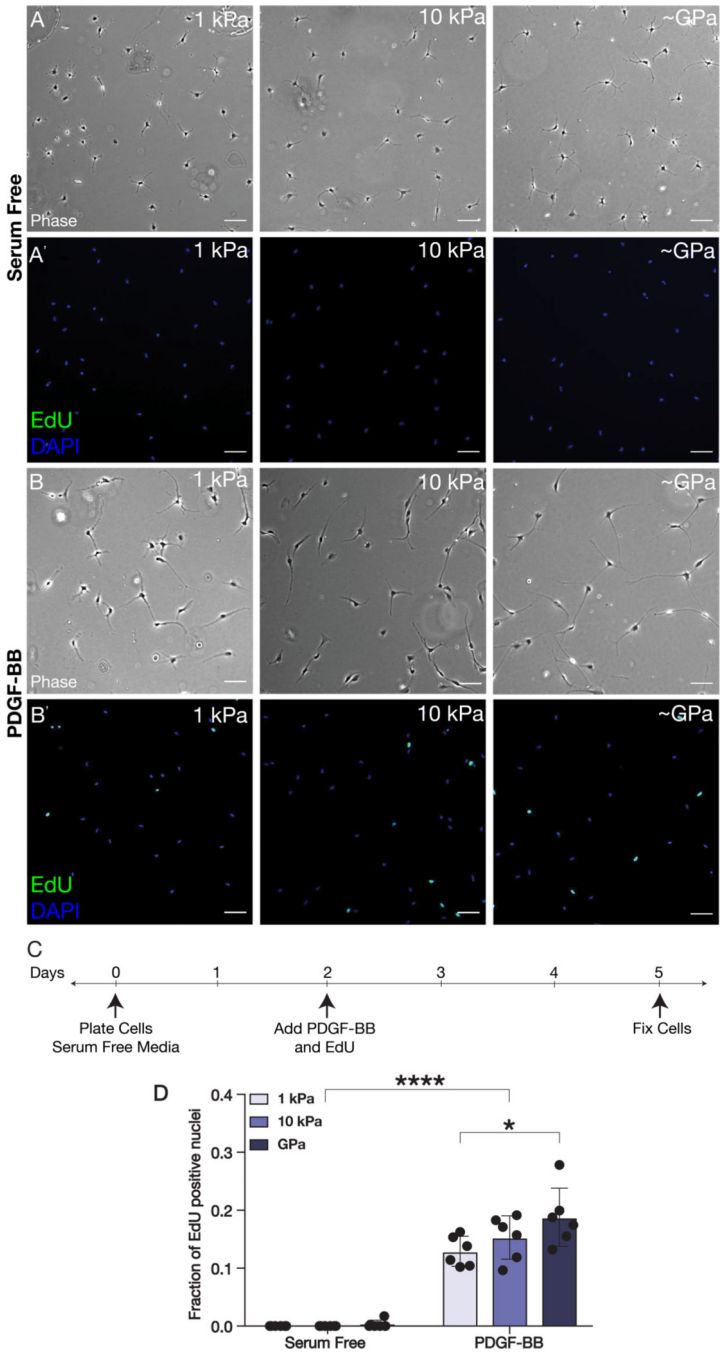

Fig. 2: PDGF-BB-mediated proliferation is modulated by substratum stiffness.

(A-B) Representative wide-field fluorescence and (A'-B') phase contrast images of corneal keratocytes cultured on substrata of different stiffnesses (1 kPa, 10 kPa, ~GPa) and stained for EdU (green) and DAPI (blue). Cells were cultured in either (A-A') serum-free conditions or (B-B') in medium containing PDGF-BB. Scale bars, 100 μm. (C) Experimental timeline. Cells were pulsed with EdU and treated with PDGF-BB for 72 hr. (D) Quantification of EdU incorporation. Error bars represent mean ± s.d. for n = 6 substrates from 3 experimental

replicates. A two-way ANOVA with a Tukey post-hoc test was used to evaluate significance among groups (*, $p < 0.05$; ****, $p < 0.0001$).

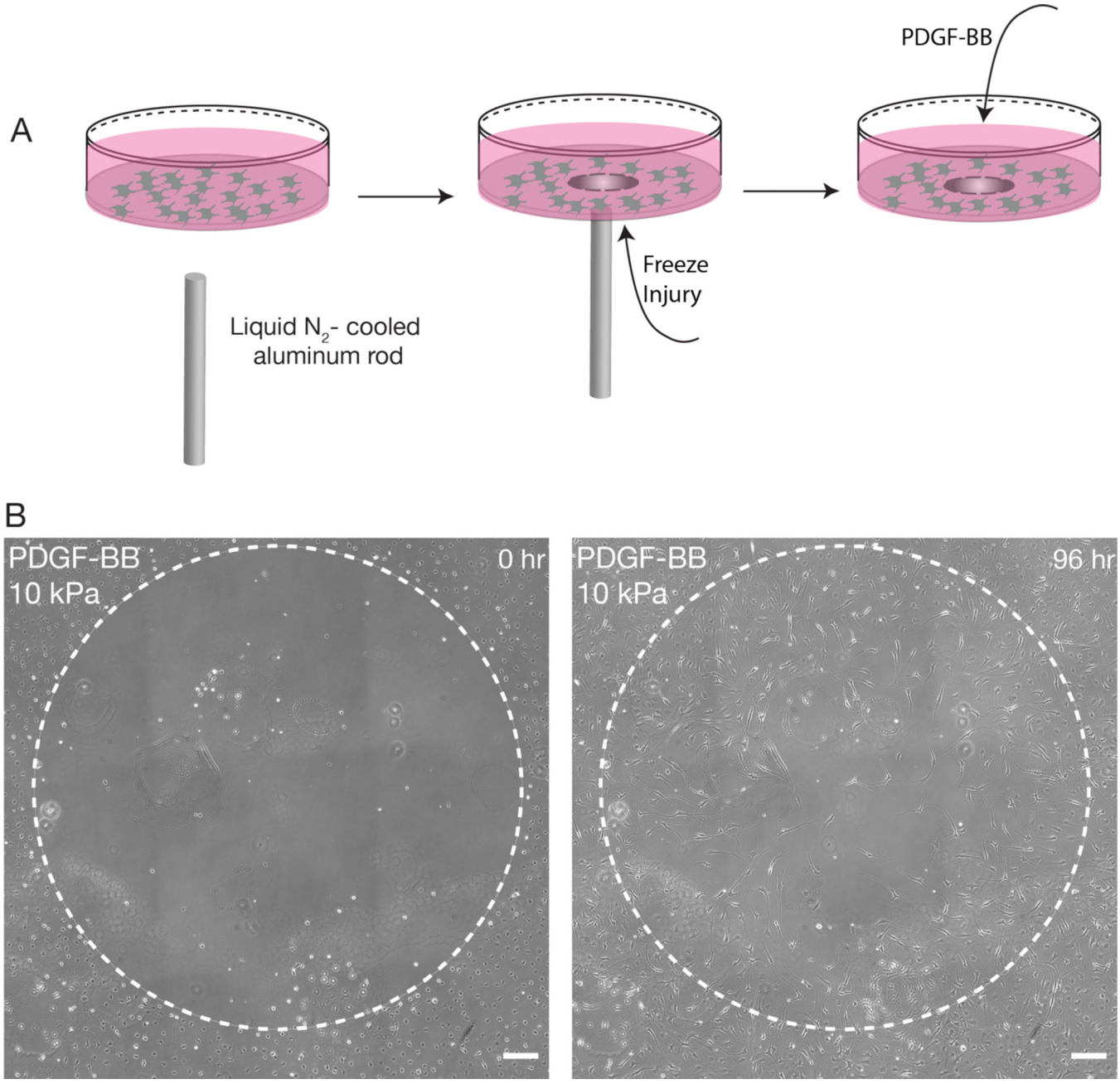

Fig, 3: Freeze injury assay induces a circular decellularized wound on PA substrata.

(A) Schematic overview of freeze injury experiment. A liquid nitrogen-cooled rod is used to create a circular freeze injury within a confluent monolayer of corneal keratocytes. (B) Representative phase contrast images of a freeze injury on a stiff (10 kPa) PA substratum after 0 and 96 hr of time-lapse culture. Note that keratocytes have migrated into the decellularized region. Scale bar, 200 μm.

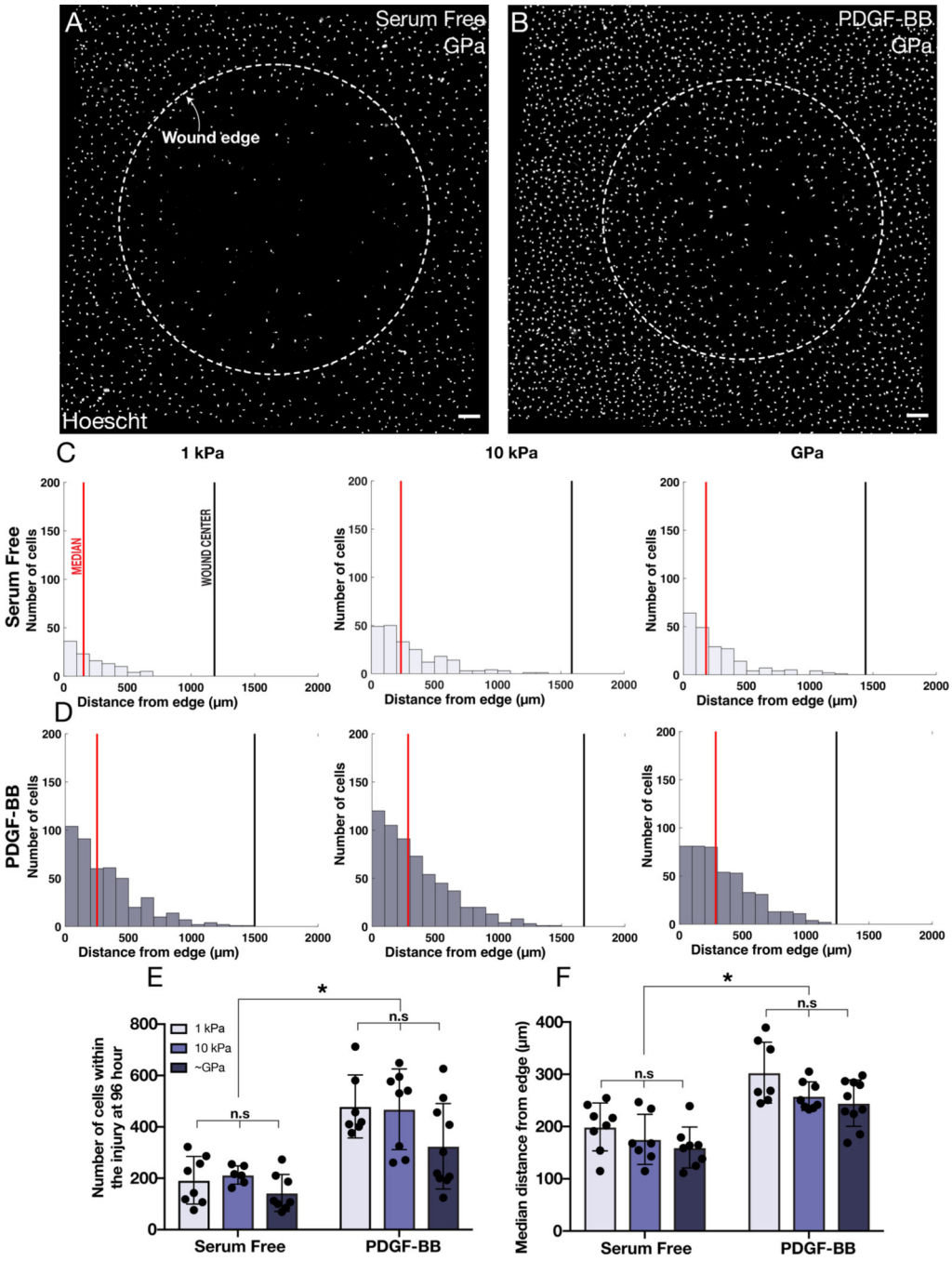

Fig. 4: Substratum stiffness does not influence how the repopulation of circular freeze injuries.

(A-B) Representative wide-field fluorescence images of Hoechst-stained nuclei after 96 hr of culture following freeze injury. Cells were cultured in either (A) serum-free conditions or (B) in medium containing PDGF-BB. Dashed white lines indicate initial wound boundaries. Scale bars, 200 μm. (C-D) Representative histograms showing the distance of cell nuclei from the initial wound border after 96 hr of culture on substrata of varying stiffnesses. Red solid lines indicate the median distance of nuclei from the wound border, and the solid black line indicates the center of the wound. (E-F) Quantification of the (E) number of the nuclei

present within each wound, as well as the (F) average median distance of the nuclei from the wound border. Error bars represent mean ± s.d. for n = 10 substrates from 10 experimental replicates. A two-way ANOVA with a Tukey post-hoc test was used to evaluate significance among groups (*, $p < 0.05$; n.s, not significant).

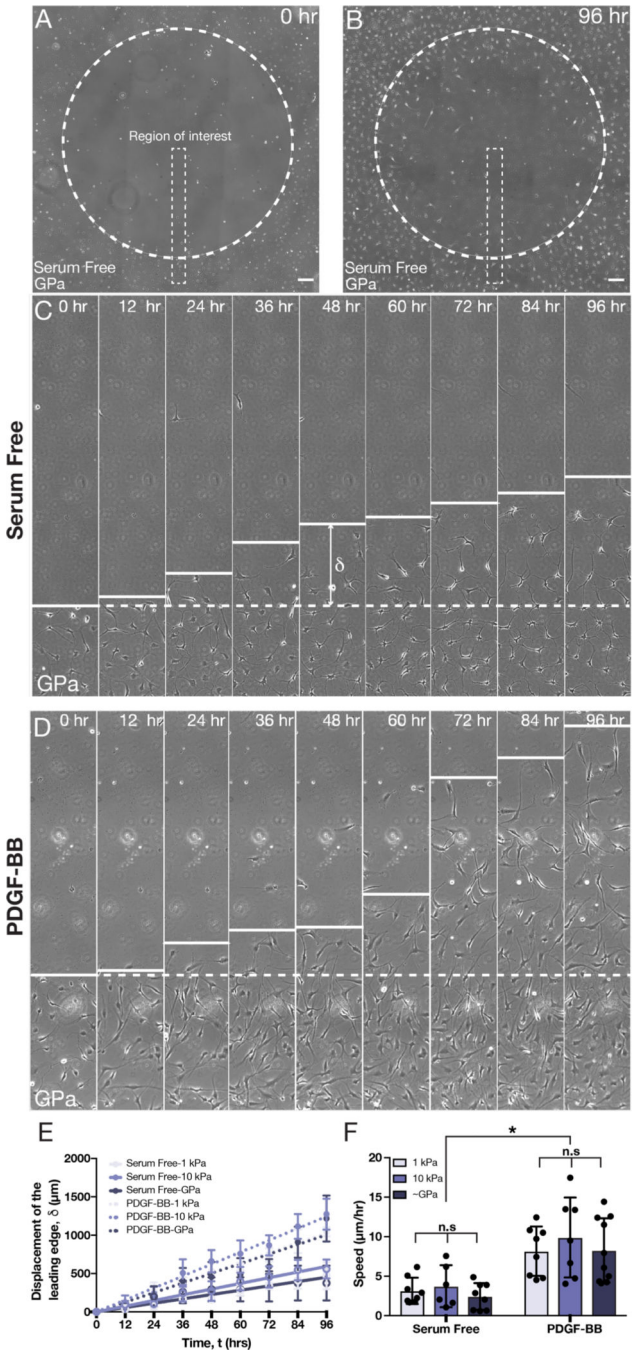

Fig. 5: Substratum stiffness does not modulate rates of wound closure in the presence of PDGF-BB.

(A) Representative phase contrast image of a freeze injury on a collagen-coated glass coverslip (~GPa) after (A) 0 and (B) 96 hr of culture. Scale bars, 200 μm. (C-D) Representative kymographs showing aggregate cell motion within thin regions of interest (as indicated in panels A & B). Cells were cultured in either (C) serum-free conditions or (D) in medium supplemented with PDGF-BB. Dashed white line indicates the initial wound border, and δ indicates the displacement of the wound edge. (E-F) Quantification of (E) the motion of wound edge, as well as (F) the speed of wound closure, on substrata of varying stiffnesses

in either the presence or absence of PDGF-BB. Error bars represent mean ± s.d. for n = 10 substrates from 10 experimental replicates. A two-way ANOVA with a Tukey post-hoc test was used to evaluate significance among groups (*, $p < 0.05$; n.s, not significant).

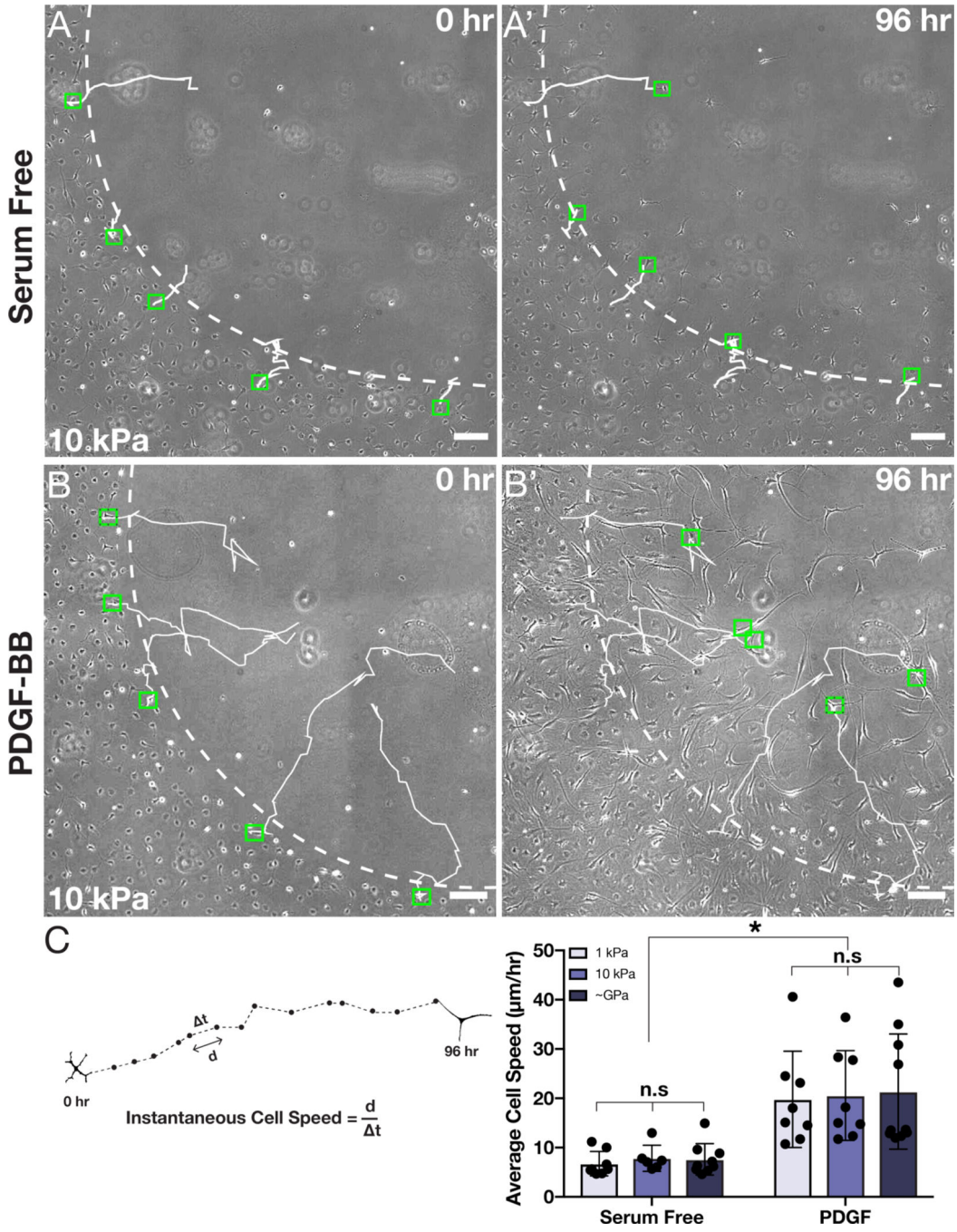

Fig. 6: Tracked motion of individual keratocytes is not modulated by substratum stiffness.

(A-B) Representative phase contrast images of cells migrating into a freeze injury in either (A) serum-free medium or (B) medium supplemented with PDGF-BB. Individual tracks are shown at either (A,B) 0 hr or at (A',B') 96 hr of culture. The dashed white lines indicate the initial wound border, the solid white lines indicate tracks of individual cells, and the green boxes designate the initial and final positions of each tracked cell. Scale bars, 100 μm. (C) Quantification of average cell speed during wound closure on substrata of different stiffnesses in either the presence or absence of PDGF-BB. Error bars represent mean ±

s.d. for n = 10 substrates from 10 experimental replicates. A two-way ANOVA with a Tukey post-hoc test was used to evaluate significance among groups (*, $p < 0.05$; n.s., not significant).